

DISCONTINUOUS OPERATION FOR PRECODED G.FAST

Rainer Strobel*[†], Wolfgang Utschick*

*Fachgebiet Methoden der Signalverarbeitung
Technische Universität München, 80290 München
{rainer.strobel,utschick}@tum.de

[†]Intel Connected Home Division
85579 Neubiberg
rainer.strobel@intel.com

ABSTRACT

Energy efficiency is besides higher data rates a key to success of the next generation copper access technology, G.fast [1]. Power consumption targets are not only driven by government requirements, but also by the need for access nodes without local power supply, which are fed from the subscriber via reverse power feeding (RPF). G.fast introduces discontinuous operation (DO) to reduce power consumption by switching lines on and off on a short time scale.

Implementing DO in combination with precoding requires to maintain precoding performance on active lines while other lines are discontinued. This paper investigates G.fast DO in combination with linear and nonlinear precoding. Spectrum and framing optimization for DO is discussed. Implementation approaches are compared in terms of complexity and power saving capabilities, considering realization aspects as well as standard-related limitations.

Index Terms— Precoding, Digital Subscriber Line, Discontinuous Operation, G.fast, Energy Efficiency

1. INTRODUCTION

Discontinuous operation [2] is a key to make G.fast a low-power consumption technology that supports RPF. Besides RPF, there are governmental requirements to reduce power consumption of network equipment [3]. In discontinuous operation, the transceiver power consumption shall scale with the current data rate. This is achieved by switching analog and digital transceiver components into low-power mode on a per-symbol basis with respect to the data traffic.

Linear [4] or nonlinear [5] precoding are used to maintain G.fast performance in multi-line systems. This paper discusses DO in combination with linear and nonlinear zero-forcing precoding. Implementation approaches are compared in terms of performance and complexity. Spectrum and framing optimization are discussed.

2. SYSTEM MODEL

The key features of G.fast in the FTTdp (fiber to the distribution point) network are summarized in [6] using a frequency spectrum from 2 MHz to 106 or 212 MHz with DMT multi-carrier modulation and synchronized time division duplexing. The FTTdp network consists of a fiber link to a reverse powered distribution point unit (DPU) which is connected to the customer premises equipment (CPE) via copper wires of the telephone network.

Each subscriber uses the subcarriers $k = 1, \dots, K$ for data transmission over the crosstalk channel described by the matrix

This work has been founded by the research project “FlexDP - Flexible Breitband Distribution Points”, funded by the Bayerische Forschungsstiftung.

$\mathbf{H}^{(k)} \in \mathbb{C}^{L \times L}$ for subcarrier k and a system with L lines. The linear precoder matrix $\mathbf{P}^{(k)} \in \mathbb{C}^{L \times L}$ at the DPU is used to pre-compensate crosstalk between the lines. The Tomlinson Harashima (TH) precoder [7], [8] uses a strictly lower triangular feed-back matrix $\mathbf{F}^{(k)} \in \mathbb{C}^{L \times L}$ and a modulo operation $\text{mod}(\cdot)$ [5] in addition for nonlinear precoding.

The gain-scaling is collected in diagonal matrices $\mathbf{S}^{(k)} = \text{diag}(s_1^{(k)}, \dots, s_L^{(k)}) \in \mathbb{R}^{L \times L}$. The operation $\text{diag}(\cdot)$ transforms a vector into a diagonal matrix and a diagonal matrix into a vector. The receivers apply the diagonal equalizer $\mathbf{G}^{(k)} = \text{diag}(g_1^{(k)}, \dots, g_L^{(k)}) \in \mathbb{C}^{L \times L}$ to compensate direct channel distortion.

The downstream model for linear precoding is described by

$$\mathbf{y}^{(k)} = \mathbf{P}^{(k)} \mathbf{S}^{(k)} \mathbf{u}^{(k)} \quad (1)$$

$$\hat{\mathbf{u}}^{(k)} = \mathbf{S}^{(k),-1} \mathbf{G}^{(k)} \left(\mathbf{H}^{(k)} \mathbf{y}^{(k)} + \mathbf{n}^{(k)} \right) \quad (2)$$

for each subcarrier k . The transmit and receive signal vectors are $\mathbf{u}^{(k)} \in \mathbb{C}^L$ and $\hat{\mathbf{u}}^{(k)} \in \mathbb{C}^L$, respectively. $\mathbf{y}^{(k)} \in \mathbb{C}^L$ is the DPU output signal. The transmit signals are assumed to be statistically independent, zero-mean, unit power QAM (quadrature amplitude modulation) signals with $b_l^{(k)}$ bits modulated on carrier k and line l . The receivers experience additive white Gaussian noise (AWGN) $\mathbf{n}^{(k)} \sim \mathcal{N}_{\mathbb{C}}(\mathbf{0}, \sigma^2 \mathbf{I})$ with noise variance σ^2 . The nonlinear precoder implements the signal processing steps

$$\mathbf{u}_{\text{back}}^{(k)} = \mathbf{F}^{(k)} \mathbf{u}_{\text{mod}}^{(k)}, \quad (3)$$

$$\mathbf{u}_{\text{mod}}^{(k)} = \text{mod} \left(\mathbf{u}_{\text{back}}^{(k)} + \mathbf{S}^{(k)} \mathbf{u}^{(k)} \right), \quad (4)$$

$$\mathbf{y}^{(k)} = \mathbf{P}^{(k)} \mathbf{u}_{\text{mod}}^{(k)} \quad (5)$$

with the intermediate signal vectors $\mathbf{u}_{\text{back}}^{(k)} \in \mathbb{C}^L$ and $\mathbf{u}_{\text{mod}}^{(k)} \in \mathbb{C}^L$. Details on linear and non-linear zero-forcing (ZF) precoding for G.fast are discussed in [9] and [10].

3. DISCONTINUOUS OPERATION

Due to the reverse power feeding architecture of FTTdp [11], low power consumption of the G.fast equipment at any time is very important. This is achieved with discontinuous operation.

3.1. Discontinuous Operation and Precoding

The combination of precoding and discontinuous operation has been studied first in [12] for linear and nonlinear precoding and further investigated in [2] for linear precoding. G.fast links using DO are only active during the time that is required to send the data. There are two different types of symbols which do not carry user data. The

idle symbol, where no data is modulated, but the transmitter remains active for crosstalk cancellation on other lines and the quiet symbol, which allows switching analog and digital front-end components of the corresponding line into low power mode. Fig. 1 illustrates the difference between idle and quiet symbols for precoding.

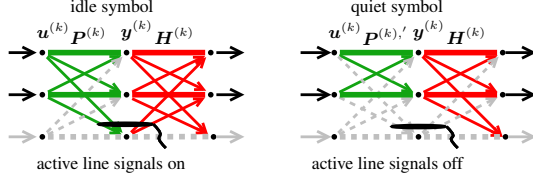


Fig. 1. Idle and quiet symbols in discontinuous operation

The highest power saving is achieved with quiet symbols, because analog front-end and line driver are major power consumers in a G.fast system and do not scale with transmit signal strength.

Without loss of generality, the transmit signal vectors are separated into an active lines signal vector \mathbf{u}_a and a discontinued lines signal vector $\mathbf{u}_d^{(k)} = \mathbf{0}$ such that the overall signal is $\mathbf{u}^{(k)} = [\mathbf{u}_a^{(k),T}, \mathbf{u}_d^{(k),T}]^T$. The same holds for the precoder output signal vector $\mathbf{y}^{(k)} = [\mathbf{y}_a^{(k),T}, \mathbf{y}_d^{(k),T}]^T$.

The channel matrix $\mathbf{H}^{(k)}$ and the precoder matrix $\mathbf{P}^{(k)}$ are accordingly partitioned into four block matrices

$$\mathbf{P} = \begin{bmatrix} \mathbf{P}_{aa} & \mathbf{P}_{ad} \\ \mathbf{P}_{da} & \mathbf{P}_{dd} \end{bmatrix}, \mathbf{H} = \begin{bmatrix} \mathbf{H}_{aa} & \mathbf{H}_{ad} \\ \mathbf{H}_{da} & \mathbf{H}_{dd} \end{bmatrix}, \mathbf{G} = \begin{bmatrix} \mathbf{G}_{aa} & \mathbf{G}_{ad} \\ \mathbf{G}_{da} & \mathbf{G}_{dd} \end{bmatrix}. \quad (6)$$

Assuming zero-forcing precoding,

$$\mathbf{G}^{(k)} \mathbf{H}^{(k)} \mathbf{P}^{(k)} = \mathbf{I} \quad (7)$$

holds when all lines are active. For a quiet symbol, not only $\mathbf{u}_d^{(k)} = \mathbf{0}$, but also $\mathbf{y}_d^{(k)} = \mathbf{0}$ must hold. This requires different precoder coefficients $\mathbf{P}_{aa}^{(k),'}$ to satisfy the zero-forcing condition.

$$\mathbf{G}_{aa}^{(k)} \mathbf{H}_{aa}^{(k)} \mathbf{P}_{aa}^{(k),'} = \mathbf{I}. \quad (8)$$

[2] shows that ignoring the coefficient change causes a significant performance drop.

Coefficient Update (CU Linear): The new precoder coefficients to satisfy (8) are obtained by

$$\mathbf{P}_{aa}^{(k),'} = \mathbf{P}_{aa}^{(k)} - \mathbf{P}_{ad}^{(k)} \mathbf{P}_{dd}^{(k),-1} \mathbf{P}_{da}^{(k)}. \quad (9)$$

Compared to the number of compute operations to be done for the precoding itself, this operation may dominate the compute requirements. Precoding of one symbol with K subcarriers and L lines requires $N_{\text{mac}} = L^2 K$ multiply-accumulate (MAC) operations.

Assuming L_a active and L_d discontinued lines, the number of compute operations for the precoder update is $N_{\text{mac}} = L_a L_d L_d + L_d L_d L_a + N_{\text{inv}}(L_d)$. The number of operations for matrix inversion of \mathbf{P}_{ij} is $N_{\text{inv}}(L_d)$. It depends on the algorithm, but in most cases, matrix inversion has cubic complexity.

Coefficient Update (CU TH): For TH ZF precoding, a correction can be done similar to Eq. (9) for linear ZF precoding.

Mode	Compute Operations per symbol
Linear Prec.	$L^2 K$
SU (linear), CA	no additional complexity
CU (linear), 1 line	$((L-1)^2 + (L-1)) K$
TH Prec.	$(L^2 + L(L-1)/2) K$
CU (TH), 1 line	$(2(L-1)^2 + N_{\text{inv}}(L_a)) K$

Table 1. Discontinuous operation precoding complexity

The correction is applied to the forward matrix $\mathbf{P}^{(k)}$ as in Eq. (5). The update is given by

$$\mathbf{P}_{aa}^{(k),'} = \mathbf{P}_{aa}^{(k)} + \mathbf{H}_{aa}^{(k),-1} \mathbf{H}_{ad}^{(k)} \mathbf{P}_{da}^{(k)}. \quad (10)$$

The feedback matrix $\mathbf{F}^{(k)}$ in the nonlinear part of the precoder as in Eq. (3) and (4) is not changed. The nonlinear operation implies an encoding order. For DO it is required that the line, which is discontinued first, is encoded last. With this approach, the nonlinear operation output $\mathbf{u}_{\text{mod}}^{(k)}$ is zero for discontinued lines.

The TH ZF operation is more complex than linear ZF precoding, requiring $N_{\text{mac}} = (L^2 + \frac{L(L-1)}{2}) K$ compute operations to precode one symbol plus the modulo operations. The precoder correction of Eq. (10), requires $N_{\text{mac}} = 2L_a L_d L_d + N_{\text{inv}}(L_a)$ operations.

Signal Update (SU Linear): An alternative DO solution is available for linear ZF precoding by changing the signal processing steps in DO rather than a coefficient update. The DO output signal is calculated using the normal operation coefficients according to

$$\mathbf{y}_a = \mathbf{P}_{aa} \mathbf{u}_a - \mathbf{P}_{ad} \mathbf{P}_{dd}^{-1} \mathbf{P}_{da} \mathbf{u}_a \quad (11)$$

instead of Eq. (1). With the assumption, that the matrix inversion \mathbf{P}_{dd}^{-1} can be approximated by the corresponding first order approximation, the following simplified approach can be implemented

$$\mathbf{y}_a = \mathbf{P}_{aa} \mathbf{u}_a + \mathbf{P}_{ad} \tilde{\mathbf{P}}_{dd} \mathbf{P}_{da} \mathbf{u}_a. \quad (12)$$

where $\tilde{\mathbf{P}}_{dd} = \mathbf{P}_{dd} - 2\mathbf{I}_{L_d}$. The approximation assumes that the precoder is scaled to satisfy $\mathbf{P}_{ad} \approx \mathbf{I}$.

Crosstalk Avoidance (CA Linear/TH): The lowest complexity solution to DO is the crosstalk avoidance scheme, where only one line transmits at a time [1]. Crosstalk avoidance allows additional power saving because crosstalk cancellation is not required during that time and no coefficient update is needed. Due to the fact that only one line is active in DO, this line achieves a high peak rate because no crosstalk is present. But when multiple lines request high data rates, the system is forced to keep all lines in the normal operation mode with high power consumption.

Table 1 summarizes the worst case number of MAC operations per symbol for different precoding and DO implementations. Coefficient updates are restricted to one discontinuing line per symbol.

3.2. G.fast Framing

G.fast uses time division duplexing (TDD) to separate upstream and downstream. Fig. 2 illustrates the structure of TDD frames with DO.

Each data frame starts with the RMC (robust management channel) symbol, followed by a downstream (DS) section, 1/2 symbol gap, the upstream (US) section, another 1/2 symbol gap and another DS section. DS and US phase are divided into a normal operation interval (NOI) and a discontinuous operation interval (DOI). During NOI, all links are active and operate at rate-optimized settings.

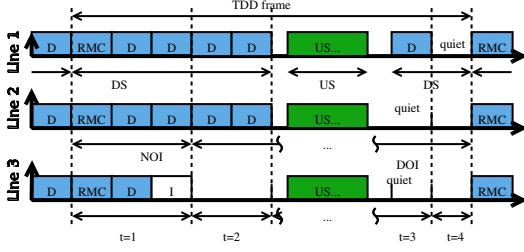


Fig. 2. G.fast framing with idle (I) and data (D) symbols

During DOI, the lines may discontinue transmission, depending on the actual data traffic. The bit loading $\hat{b}_l^{(k)}$ as well as the gain values $s_l^{(k)}$ are different for NOI ($\hat{b}_{\text{NOI},l}^{(k)}, s_{\text{NOI},l}^{(k)}$) and DOI ($\hat{b}_{\text{DOI},l}^{(k)}, s_{\text{DOI},l}^{(k)}$). These settings are exchanged between DP and CPE in advance to allow a fast switching between them. Using only these two settings does not allow the use of optimized parameters in DOI, because this may require different bit and gain values when lines discontinue.

The frame format is controlled within the RMC, which defines the number of transmitted symbols and their position in the DOI. For framing optimization, each frame is further partitioned into configurations $t = 1, \dots, T$, as shown in Fig. 2, where a change of t indicates that lines are enabled or discontinued.

3.3. Spectral Constraints for NOI and DOI

G.fast is subject to two power constraints, the per-line spectral mask and a per-line sum-power constraint as defined in [13]. Spectrum optimization for linear and nonlinear ZF precoding in G.fast is discussed in [9] and [10].

With DO, the precoder $\mathbf{P}^{(k),[t]}$ depends on the position t in the TDD frame as indicated in Fig. 2. For every index $t = 2, \dots, T$ in the DOI, the precoder changes. The spectral mask constraint for NOI is given by

$$\text{diag} \left(\mathbf{P}^{(k),[1]} \mathbf{S}_{\text{NOI}} \mathbf{S}_{\text{NOI}}^{\text{H}} \mathbf{P}^{(k),[1],\text{H}} \right) \leq \mathbf{p}_{\text{mask}} \forall k = 1, \dots, K \quad (13)$$

and a per-line sum-power constraint is

$$\sum_{k=1}^K \text{diag} \left(\mathbf{P}^{(k),[1]} \mathbf{S}_{\text{NOI}} \mathbf{S}_{\text{NOI}}^{\text{H}} \mathbf{P}^{(k),[1],\text{H}} \right) \leq \mathbf{p}_{\text{sum}}. \quad (14)$$

Standard G.fast is limited to a single gain setting $\mathbf{S}_{\text{DOI}}^{(k)}$, which shall satisfy the constraints for any selection of active lines during the DOI, $t > 1$. This gives the constraints for spectral mask

$$\text{diag} \left(\mathbf{P}'_{\text{aa}}{}^{(k),[t]} \mathbf{S}_{\text{aa,DOI}}^{(k),\text{H}} \mathbf{S}_{\text{aa,DOI}}^{(k)} \mathbf{P}'_{\text{aa}}{}^{(k),[t],\text{H}} \right) \leq \mathbf{p}_{\text{mask}} \quad (15)$$

$$\forall k = 1, \dots, K \quad \forall t = 2, \dots, T,$$

and per-line sum-power

$$\sum_{k=1}^K \text{diag} \left(\mathbf{P}'_{\text{aa}}{}^{(k),[t]} \mathbf{S}_{\text{aa,DOI}}^{(k),\text{H}} \mathbf{S}_{\text{aa,DOI}}^{(k)} \mathbf{P}'_{\text{aa}}{}^{(k),[t],\text{H}} \right) \leq \mathbf{p}_{\text{sum}} \quad (16)$$

$$\forall t = 2, \dots, T$$

during DOI. With the constraint set of Eq. (15) and (16), the optimization according to [10] is applied. The constraint set is created over all relevant configurations $t = 1, \dots, T$, which is a subset of all possible configurations $T \leq 2^L$.

3.4. Data Rates in DOI

Besides the gain values $s_l^{(k),[t]}$, the bit allocation per carrier $\hat{b}_l^{(k),[t]}$ also depends on the configuration t in the G.fast system with DO. With a given signal-to-noise-ratio $\text{SNR}_l^{(k),[t]}$, the achievable number of bits per channel use $b_l^{(k),[t]}$ for line l and carrier k reads as

$$b_l^{(k),[t]} = \log_2 \left(1 + \frac{\text{SNR}_l^{(k),[t]}}{\Gamma} \right). \quad (17)$$

with the SNR gap Γ to accommodate coding gain, non-Gaussian modulation and to achieve the desired bit error rate. The SNR is derived from the receiver error $\mathbf{e}^{(k)} = \hat{\mathbf{u}}^{(k)} - \mathbf{u}^{(k)}$, given by

$$\mathbf{e}^{(k)} = \mathbf{S}^{(k),-1} \mathbf{G}^{(k)} \left(\mathbf{H}^{(k)} \mathbf{P}^{(k)} \mathbf{S}^{(k)} \mathbf{u}^{(k)} + \mathbf{n}^{(k)} \right) - \mathbf{u}^{(k)}. \quad (18)$$

Assuming that the transmit signal $\mathbf{u}^{(k)}$ is a unit power signal and further assuming that the zero-forcing condition is satisfied, the error reduces to $\mathbf{e}^{(k)} = \mathbf{S}^{(k),-1} \mathbf{G}^{(k)} \mathbf{n}^{(k)}$ and the corresponding SNR $\text{SNR}_l^{(k),[t]}$ of line l and carrier k is given by

$$\text{SNR}_l^{(k),[t]} = \frac{1}{\mathbb{E} \left[|e_l^{(k),[t]}|^2 \right]}. \quad (19)$$

With the limitation to one bit allocation table $\hat{b}_{\text{NOI},l}^{(k)}$ for the NOI and one for DOI $\hat{b}_{\text{DOI},l}^{(k)}$, they are derived as follows

$$\hat{b}_{\text{NOI},l}^{(k)} = \min \left(\left\lfloor b_l^{(k),[t=1]} \right\rfloor, b_{\text{max}} \right), \quad (20)$$

$$\hat{b}_{\text{DOI},l}^{(k)} = \min_{t=2, \dots, T} \left(\left\lfloor b_l^{(k),[t]} \right\rfloor, b_{\text{max}} \right) \quad (21)$$

which also incorporates the upper bound $b_l^{(k)} \leq b_{\text{max}}$ on the constellation size and the fact that only an integer number of bits is loaded. The corresponding line rate is

$$R_l = \frac{\eta}{t_{\text{sym}}} \sum_{k=1}^K \hat{b}_l^{(k)} - R_{\text{oh}}, \quad (22)$$

with a symbol duration t_{sym} including the cyclic prefix and windowing, an efficiency factor η and the overhead channel rate R_{oh} which account for the losses due to communication protocol, framing overhead and management communication [9].

3.5. Framing Optimization

Optimized G.fast framing for DO is formulated as a linear program to derive the transmit time (number of symbols) for each configuration t . For each configuration t , the corresponding rates are collected in a rate vector $\mathbf{r}^{[t]} \in \mathbb{R}^L$. From the rate vectors, a rate matrix $\mathbf{R} \in \mathbb{R}^{L \times T+1}$ is formed according to

$$\mathbf{R} = \left[\mathbf{r}^{[t=1]}, \mathbf{r}^{[t=2]}, \dots, \mathbf{r}^{[t=T]}, \mathbf{0} \right] \quad (23)$$

where the first column corresponds to the NOI and with the all-zeros vector $\mathbf{0}$ as last entry. For CU and SU, the links are deactivated sequentially. Therefore, the rate matrix \mathbf{R} forms a triangular matrix plus the zero vector. For CA, only one link at a time is active in the DOI which gives a diagonal matrix for the DOI part of \mathbf{R} .

Furthermore, the time vector $\boldsymbol{\tau} \in \mathbb{R}_+^{T+1}$ is defined, where $\sum_{i=1}^{T+1} \tau_i = 1$ holds. The actual link rates vector \boldsymbol{r} is then given by

$$\boldsymbol{r} = \boldsymbol{R}\boldsymbol{\tau} \quad (24)$$

The power consumption of a configuration can be derived by the power weight vector $\boldsymbol{c} \in \mathbb{R}^{T+1}$

$$c_t = \sum_{l=1}^L \rho_l^{[t]} \quad (25)$$

which is the sum of the individual power consumption values $\rho_l^{[t]}$ of each line l during configuration t . Consequently, the framing optimization is described by the following linear program

$$\begin{aligned} \min_{\boldsymbol{\tau}} \boldsymbol{c}^T \boldsymbol{\tau} \quad & \text{s.t. } \tau_i \geq 0 \forall i = 1, \dots, T+1 \\ & \text{s.t. } \sum_{i=1}^{T+1} \tau_i = 1 \quad \boldsymbol{R}\boldsymbol{\tau} \geq \boldsymbol{r}_{\min} \end{aligned} \quad (26)$$

such that the actual data rates are greater or equal to a required rate vector \boldsymbol{r}_{\min} , which is provided from the dynamic resource allocation (DRA) [14]. $\boldsymbol{\tau}$ is quantized to match the number of symbols N_{sym} in the TDD frame $\hat{\boldsymbol{\tau}} = \lceil \boldsymbol{\tau} \cdot N_{\text{sym}} \rceil$.

Power consumption is implementation dependent. Therefore, a simplified model is used by choosing $\rho_l^{[t]} = 0$ for quiet symbols and $\rho_l^{[t]} = 1$ for idle and data symbols. The per-line average power consumption is $\rho_l = \sum_{t=1}^T \tau_t \rho_l^{[t]}$. $\rho_l = 1$ corresponds to a link that is always active.

3.6. Avoid Bad Combinations

As mentioned in Sec. 3.3 and 3.4, standard G.fast [1] uses the same bit allocation $\hat{b}_l^{(k)}$ and gains $\boldsymbol{S}^{(k)}$ throughout the DOI. It is selected with respect to the worst case SNR and precoder. Therefore, a specific selection of discontinued lines may cause a performance drop for the whole DOI. They are referred to as bad combinations t_{bad} .

The bad combinations can be defined such that the rate is below a certain percentage α_{bad} of the NOI rate

$$t_{\text{bad}} = \left\{ t : \hat{r}_{lt} = \sum_{k=1}^K b_l^{(k),[t]} < \alpha_{\text{bad}} \sum_{k=1}^K b_l^{(k),[1]} \right\}. \quad (27)$$

Such configurations are excluded from the possible configurations $t = 1, \dots, T$ to maintain sufficient data rates in the DOI. For the simulations $\alpha_{\text{bad}} = 0.8$ is used.

4. SIMULATION RESULTS

Simulations focus on G.fast with 106 MHz profile and linear precoding with up to 16 lines. CPEs are non co-located, e.g., each line in the binder has a different length between 10 m and 400 m. Background noise of -140 dBm/Hz below 30 MHz and -150 dBm/Hz above 30 MHz is used [15]. The cable is 0.5 mm PE DTAG [16]. The transmit PSD is given by [13] with 4 dBm transmit power.

Fig. 3 compares the achievable peak rates in DOI with the NOI data rates vs. line length. The DOI rates do not reflect the rates which are available to the subscriber, because the actual data rate is a mix of NOI and DOI rate. But high data rates in DOI allow to transmit in a shorter time frame, allowing more power saving.

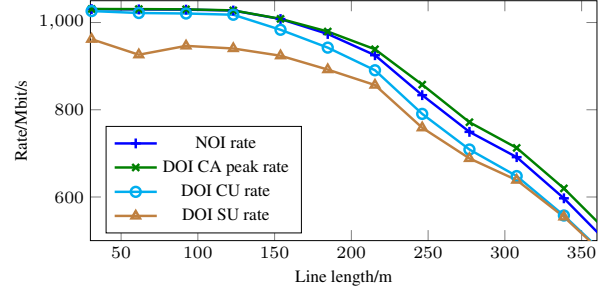


Fig. 3. Rate vs. reach of NOI and DOI rates for a 12 lines DPU

Highest peak rates in DOI (even higher than NOI rates) are achieved by CA because no crosstalk is present. However, the high peak rates are only available to one line at a time. CU experiences some rate loss compared to NOI, due to the single bits and gains setting within DOI. SU achieves lowest rates because of the approximated matrix inverse in Eq. (12).

Power consumption simulations are done with random target rates $0 < r_{\min,l} < r_l^{[t=1]}$ between zero and the NOI rate, where the ratio of the binder sum rate $\sum_{l=1}^L r_{\min,l}$ and the NOI sum rate $\sum_{l=1}^L R_{\text{NOI}}$ is varied between 0.1 and 0.9. Fig. 4 compares power consumption as a function of average system load.

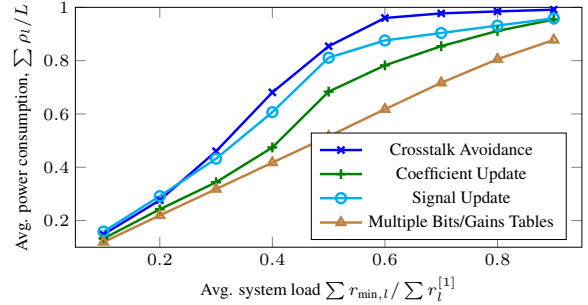


Fig. 4. Power consumption vs. load for DO with 16 lines

Removing the standard-related limitation and using different bit allocation $\hat{b}_l^{(k),[t]}$ and gains $\boldsymbol{S}^{(k),[t]}$ for each configuration t gives the lowest power consumption. Bringing the limitation to a single bits and gains table for DOI gives the CU curve. SU with approximated matrix inversion, having lower complexity, achieves less power saving. CA shows the lowest power saving at high load, but the high power saving at very low loads.

5. CONCLUSION

Discontinuous operation for G.fast is discussed in terms of possible DO implementations for downstream direction. The most power saving solution requires multiple bits and gains tables during DOI. The G.fast standard restriction to one table results in rate losses for DOI, which are tolerable for smaller DPUs up to 16 ports. Even low complexity implementations using SU or CA give good power savings for lower loads, indicating that DO can be implemented with low complexity.

6. REFERENCES

- [1] ITU-T Rec. G.9701, "Fast Access to Subscriber Terminals - Physical layer specification," ITU Recommendation, 2015.
- [2] J. Maes and C. Nuzman, "Energy efficient discontinuous operation in vectored G.fast," in *Communications (ICC), 2014 IEEE International Conference on*. IEEE, 2014, pp. 3854–3858.
- [3] European Commission Joint Research Centre, "Code of Conduct on Energy Consumption of Broadband Equipment, Version 4.1," Institute for Energy and Transport, 2013.
- [4] R. Cendrillon, M. Moonen, E. Van den Bogaert, and G. Ginis, "The linear zero-forcing crosstalk canceler is near-optimal in DSL channels," in *Global Telecommunications Conference, 2004. GLOBECOM'04.*, vol. 4, 2004, pp. 2334–2338.
- [5] G. Ginis and J. Cioffi, "Vectored transmission for digital subscriber line systems," *IEEE Journal on Selected Areas in Communications*, vol. 20, no. 5, pp. 1085–1104, 2002.
- [6] M. Timmers, M. Guenach, C. Nuzman, and J. Maes, "G.fast: evolving the copper access network," *IEEE Communications Magazine*, vol. 51, no. 8, 2013.
- [7] M. Tomlinson, "New automatic equaliser employing modulo arithmetic," *Electronics letters*, vol. 7, no. 5, pp. 138–139, 1971.
- [8] H. Miyakawa and H. Harashima, "Information transmission rate in matched transmission systems with peak transmitting power limitation," in *Nat. Conf. Rec., Inst. Electron., Inform., Commun. Eng. of Japan*, vol. 7, no. 2, 1969, pp. 138–139.
- [9] R. Strobel, M. Joham, and W. Utschick, "Achievable Rates with Implementation Limitations for G.fast-based Hybrid Copper/Fiber Networks," in *IEEE ICC 2015 SAC - Access Networks and Systems (ICC'15 (01) SAC 7-ANS)*, London, United Kingdom, Jun. 2015.
- [10] R. Strobel, A. Barthelme, and W. Utschick, "Zero-Forcing and MMSE Precoding for G.fast," in *2015 IEEE Global Communications Conference: Selected Areas in Communications: Access Networks and Systems (GC' 15 - SAC - Access Networks and Systems)*, San Diego, USA, Dec. 2015.
- [11] M. Timmers, K. Hooghe, M. Guenach, C. Stony, and J. Maes, "System design of reverse-powered G. fast," in *Communications (ICC), 2012 IEEE International Conference on*. IEEE, 2012, pp. 6869–6873.
- [12] V. Oksman and R. Strobel, "G.fast: Precoder update in support of discontinuous operation," Contribution ITU-T SG15/Q4a 2013-01-Q4-068, 2013.
- [13] ITU-T Rec. G.9700, "Fast access to subscriber terminals (FAST) - Power spectral density specification," ITU Recommendation, 2013.
- [14] F. C. Muller, C. Lu, P.-E. Eriksson, S. Host, and A. Klautau, "Optimizing power normalization for G. fast linear precoder by linear programming," in *2014 IEEE International Conference on Communications (ICC)*. IEEE, 2014, pp. 4160–4165.
- [15] L. Humphrey, "On VHF background noise assumptions for G:FAST," Contribution ITU-T SG15/Q4a C0431-E, 2013.
- [16] Broadband Forum, "TR-285 Cable Models for Physical Layer Testing of G.fast Access Network," Technical Report, 2015.